Egyptian Geophysical Society
EGS Journal, Vol. 10, No. 1, 151-161 (2012)

INTEGRATION OF LANDSAT ETM+ IMAGERY AND AIRBORNE GEOPHYSICAL DATA TO DISCRIMINATE ROCK UNITS AND RING COMPLEXES IN GEBEL EL NAQA AREA, SOUTH EASTERN DESERT, EGYPT.

S.M.M. Hanafy, M.I. Mousa and S.A. Wasfi

Nuclear Materials Authority, P.O. Box 530, El Maadi, Cairo, Egypt.

"تكامل بيانات المرئيات من نوع +ETM والبيانات الجيوفيزيائية الجوية لتمييز الوحدات الصخرية والحلقيات المعقدة فى منطقة الناقة؛ جنوب الصحراء الشرقية، مصر."

الخلاصة: أن الهدف الأساسى لهذا العمل هو عرض كيفية استخدام تكامل كل من البيانات الجيوفيزيائية وصور الأقمار الصناعية والتى تؤدى إلى تمييز و تعريف الوحدات الصخرية والحلقيات المعقدة؛ حيث تفيد الخرائط الإشعاعية فى تحديد حدود الصخور النارية والمتحولة، بالإضافة إلى ذلك تعطى الصورة الملونة والمركبة من العناصر الجيوكيميائية فى عرض واحد صورة عامة عن التوزيعات الإشعاعية لمنطقة الدراسة، لقد تم فصل الشاذات المغناطيسية الكلية المحولة إلى القطب الشمالى للأرض إلى مركبتين المتبقية القريبة من السطح والإقليمية الغائرة فى العمق، وذلك باستخدام تقنية الترشيح النطاقى لجاويس. وأيضاً تم تطبيق برنامج النمذجة التفاعلية ثنائية الأبعاد إلى حلقة الناقة المعقدة فى خط عمودى على خطوط الطيران لتحديد الشكل الاقحامى التحت السطحى. ومن تفسير المرئيات كاذبة الألوان المركبة +ETM (2,4&7) وجد انها تستطيع بسهولة تحديد الحواف للواحدات الصخرية طبقا لأختلاف الألوان والخصائص الفوتوجيولوجية ، بالإضافة إلى مرئيات النسب كاذبة الالوان المركبة (5/7,4/5,3/1) على التوالى. وقد كشفت النتائج أن الجزء الجنوبى الشرقى لمنطقة الدراسة عند جبل الواقف يظهر تناقض واضح للشيست و النيس فى الخريطة الجيولوجية مع البيانات الجيوفيزيائية حيث تعكس تركيزات إيجابية متميزة للعدد الكلى و البوتاسيوم والثوريوم مع تركيز أقل لليورانيوم بالإضافة إلى أنه يظهر منخفضاً مغناطيسياً والذى يعكس مكشف نيسوز جرانيت. وقد كشفت النتائج أن هناك اثنين من الحلقيات المعقدة تظهران فى الجزء الجنوبى لمنطقة الدراسة فى بيانات المرئيات من نوع لاندسات حيث تتميز بالشكل الدائرى و المخروطى. ويبين التفسير المغناطيسى لحلقة الناقة المعقدة بأن الشكل ثنائى الأبعاد لتركيب الحلقة المعقدة لم يقصر على القشرة العليا الهشة فقط ولكن يمكن أن يمتد خلال القشرة أيضاً. وتشير التحليلات إلاحصائية لتفسير الخطوط التركيبية لمنطقة الدراسة أن الأتجاهات السائدة بالمنطقة هى شمال شرق وشمال غرب، وشرق غرب على التوالى.

ABSTRACT: *The prime aim of this work is to demonstrate how can the integration of geophysical and satellite imagery data lead to discrimination and identification of the rock units and ring complexes. The spectrometric maps are useful to illustrate the boundaries of igneous and metamorphic rocks. The radioelement ternary map of K%, eU and eTh (in RGB) provide, on a single display, an overall picture of the radioelement distributions across the study area. Isolation of the magnetic anomalies was conducted for reduced to magnetic pole map into deep regional and shallow residual components. Forward modeling was applied only to the El Naqa ring complex. A 2-D magnetic model was used to account for the limited extent of the intruded zone perpendicular to the flight lines. From the interpretation of false colored composite images of ETM$^+$ bands 7, 4 & 2 in RGB, it can be easy to distinguish the boundaries between rock units, according to color differences and photogeological characteristics of the rocks, in addition to the band ratio combination of ratio, 5/7, 5/4, 3/1 in RGB, respectively. The results revealed that, to the southeast part of the survey area at Gebel El Waqif, the correlation between the mapped gniess and schist and the spectrometry response as recorded becomes progressively poorer. This contrast is due to distinct high total count, potassium and thorium with a lower extent for uranium and appear to be magnetically low which reflect gneissose granite exposures. There are two ring complexes, which appear at the southern part for the study area in the landsat imagery. They are characterized by their cone and circular shape. The magnetic interpretation of the El Naqa ring complex demonstrates that, the 2-D structure of the ring complexes is not restricted to the brittle upper crust but can extend through the crust as well. Statistical analyses of interpreted lineaments affecting the study area revealed that the predominant structural trends arranged in a decreasing density order are, NE-SW, NW-SE, and E-W.*

INTRUDUCTION

The study area lies at the southern part of the Eastern Desert of Egypt, between latitudes 22º 40´ and 23º 00´ N and longitudes 34º 22´ and 34º 45´E. It covers a surface area of about 1546 km^2 (Fig. 1). The area is formed mainly, from the oldest to the youngest, of gneiss, metavolcanic, granodiorite, older granite, younger granite, ring complex and Quaternary. The total area is highly affected by fault sets and joints of different trends.

Generally, the South Eastern Desert domain (SED) is characterized by the presence of highly metamorphosed and migmatized gneisses and syntectonic granitic intrusions (Akaad and El Ramly, 1960; and El Ramly, 1972). Also, the ring complexes are mainly concentrated at the South Eastern Desert,

south of latitude 25ºN, which represent young intrusions emplaced into the Precambrian crystalline Basement rocks.

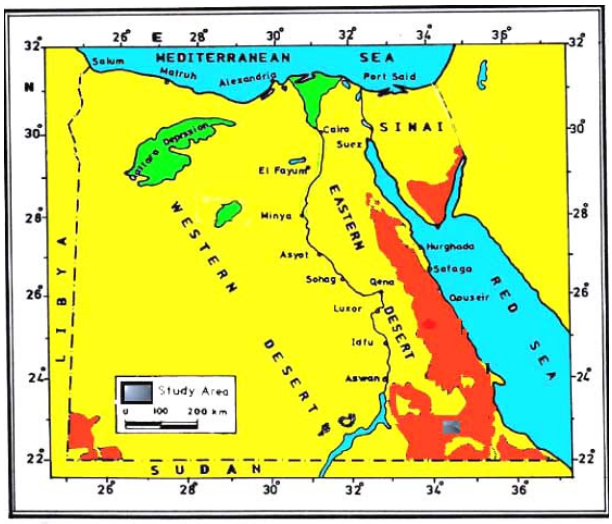

Fig. (1) Location map of the study area.

The alkaline ring complexes were emplaced in various parts of the African continent, following the Pan-African Orogeny in the Precambrian times and during one or more successive periods of Phanerozoic anorogenic magmatism (Bowden, 1985; and Vail, 1985&1989). They intrude the Upper Proterozoic metavolcanic sedimentary sequences and the Pan-African calc-alkaline orogenic-related granitoids (El Gaby et al., 1990). There are many ring complexes hosting the potentially economic rare earth mineralizations, such as Elba ring complex (Ibrahim, 1999) and radioactive anomalies in El Gezira ring complex (Farag, 1999).

The Egyptian ring complexes are formed essentially of alkaline syenites and their volcanic equivalents, where a wide range of rocks from alkaline granites to rocks composed mainly of nepheline may occur, silica and/or alumina deficiency is evident in most ring complexes (Kamel, 1991). El Ramly et al., (1970) stated that the tectonic distribution of the ring complexes in the Eastern Desert is governed by the configuration of the Basement and the Red Sea rift structures as well as the NW and the NE trends. Garson and Krs (1976) mentioned that a large-scale shear zone and deep-seated tectonic features are trending N30ºW and N60ºE, were considered to be related to the rifting and opening of the Red Sea, and the rejuvenation of these faults were accompanied by intrusions of the alkaline ring structures. Vail (1984) described the ring complexes as a group of igneous intrusives confined to two narrow bands trending N-S and ENE-WSW, which appear to be related to brittle fracturing of the cratonized Basement, after the termination of the tectonic events. The per-alkaline granites and alkaline syenite ring complexes and stock-like intrusions in the South Eastern Desert of Egypt are distributed either along the ENE lineaments representing onshore extensional faults or situated at the junction between the ENE lineaments and NNW deep-seated tectonic zones (El Ramly and Hussein, 1985). Abdel Monem et al., (1998) mentioned that, in the South Eastern Desert of Egypt, post-tectonic Phanerozoic ring complexes occur within definable linear groups, where the major faults as the Najd system in the Arabian-Nubian Shield are associated with high-level intrusions. They added in their opinion that the association of the alkaline magmatism with deep major fracture zones may suggest that, these fractures caused the lowering of pressure in zones of melting deep in the crust or upper mantle, triggering the initiation of partial melting and generating such alkaline magmas.

Generally, the lithology, especially alkaline rocks, and the structural pattern in the area are responsible for the deposition of uranium mineralization at this area. Lockwood Survey Corporation (1968) reported that, the radiometric values, ranging between 600 cps and 1000 cps, are concentrated at a large area located to the southeast of Aswan, including the studied area. The airborne radiometric survey (Aero-Service, 1984) carried out in the South Eastern Desert indicated that some of ring complexes show radioactive anomalies. El Nisr and Saleh (2001) mentioned that, the U mineralized zones in Mansouri ring were found in the alkali feldspar syenites, especially in the zones of steeply dipping intersected faults.

The ring complexes of the Eastern Desert of Egypt have ages ranging from Cambrian to Cretaceous and could be classified into four groups of Phanerozoic age (Serensits et al., 1979). They are formed essentially of alkaline syenites and their volcanic equivalents, in which a wide range of rocks varied from alkaline granites to rocks composed mainly of nepheline may occur, and the silica and / or alumina deficiency are evident in most ring complexes (Abdel Monem et al., 1998).

Field radiometric survey reveals that, the younger granitoids and ring complexes are of great interest, because they include most of the radioactive anomalies, of which some of them were found to contain uranium mineralization. Furthermore, many of them are hosts of potentially economic rare earth mineralization (e.g. U-bearing and rare earth minerals in Elba ring complex, Ibrahim, 1999; radioactive anomalies in El Gezira ring complex, Farag, 1999). Therefore, a particular attention was paid to these rocks.

GENERAL GEOLOGY

According to the Egyptian General Petroleum Corporation (EGPC) and Conoco Coral (1986), the Gebel EL Naqa area is formed from the following rock units, from oldest to youngest, (1) gneiss and schist (2) metavolcanics, (3) metasediments, (4) granodiorites and older granites, (5) younger granites, (6) ring complexes and (7) Quaternary deposits (Fig. 2).

In the area under consideration, the grey granites are widely distributed around G. El Waqif, as well as some masses within and around the ring complexes (Fig. 2).

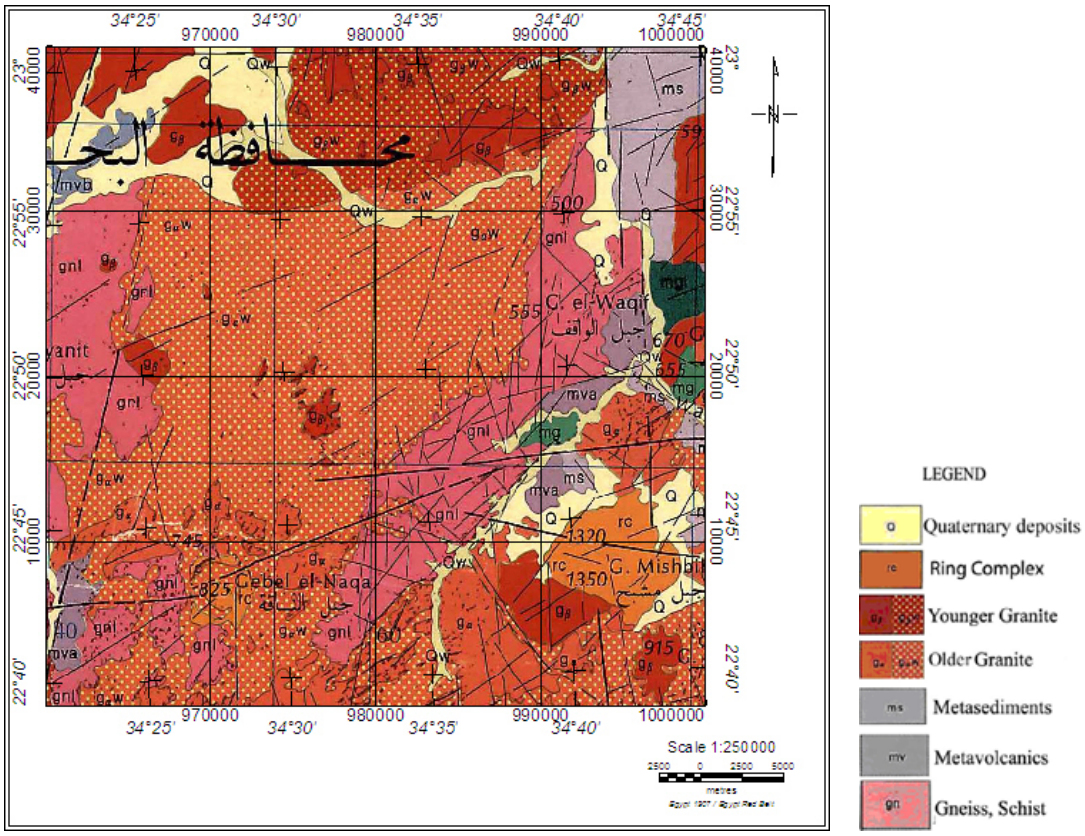

Fig. (2) Geological map of G. El Naqa area, Eastern Desert, Egypt. (Conoco, 1986).

They cover a large area and cropped out as small hills separated with broad shallow elongated wadis, sandy plains, and scattered accumulations of boulders and dike swarms. They show gradational contacts with the surrounding rocks. Gneiss and Metavolcanics possess elongated and dissected shape, with gradational and irregular contacts with the surrounding rocks. Younger granites occur as small outcrops intruding in the older granites, forming sharp contact.

Two ring complexes are outcropping within the Precambrian terrain. The first one is El Naqa ring complex, which occurs in the southwestern corner, as incomplete ring, with circular to oval - shaped outline, intruding in the older granitoids and forming sharp contact with the surrounding rocks. The second ring complex is G. Mishbih that located at the southeastern corner of the study area, with circular to oval – shaped outline.

Data Used and Transformation

Spatial integration of various data sets including the geological map, Landsat ETM$^+$ image, and airborne spectrometric and magnetic data were used for investigating the lithological discrimination and the regional structural lineaments crossing the area, as well as to delineate the anomalous zones in the study area. An airborne geophysical survey for the study area was carried out by Aero- Service, Western Geophysical Company of America in 1984, as designated as area - II (Aero- Service 1984).

This survey involves aerospectrometric and aeromagnetic data. The mapped data show the apparent surface concentrations of the radioelement, Potassium (K in %), equivalent Uranium (eU in ppm) and equivalent Thorium (eTh in ppm), in addition to the integral gamma-ray activity (Tc in µR/h), as well as total magnetic field intensity measurements are reduced to the north pole (RTP in nT). Processing of these data was carried out using Oasis montage data processing and analysis system (Geosoft, 2002).

The spectrometry maps are useful to enhance the boundaries of igneous and metamorphic rocks. The total count (Fig. 3), potassium (Fig. 4), uranium (Fig. 5) and thorium (Fig. 6) maps covering the study area, show highly variable data due to the diversity of surface lithologies. These values range from very low recorded over the metasediments and metavolcanics, to strong spectrometric response found over the younger granites. Therefore, such distribution has been chosen as an appropriate model for the radioelement ternary map (Fig. 7). It combines the data for K% (in red), eU (in green) and eTh (in blue) and provides only one display as an overall picture of the radioelements distribution in the study area. This map offers much in terms of lithologic discrimination, based on color differences.

The spectral analysis using MAGMAP 2D-FFT system supports the common Fourier domain filters to the aeromagnetic gridded data. The magnetic data were transformed to the wave number domain.

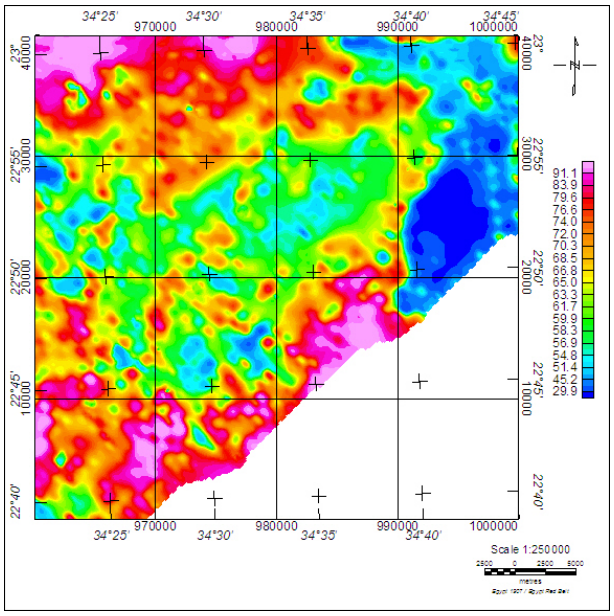

Fig. (3) Total count map of the studied area.

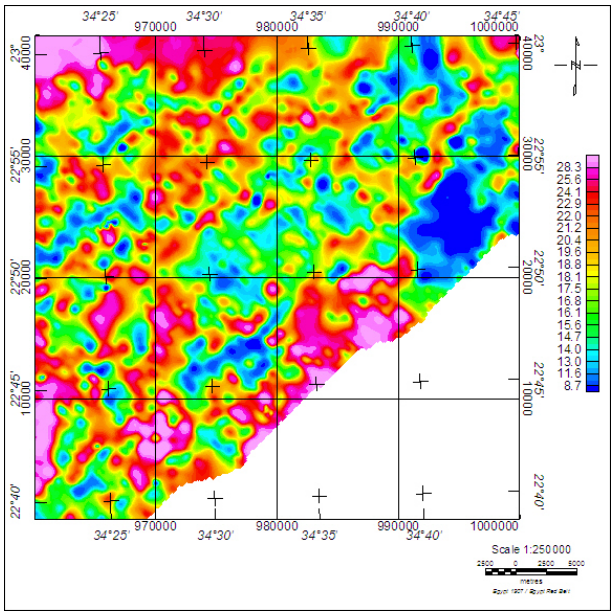

Fig. (5) Uranium map of the studied area.

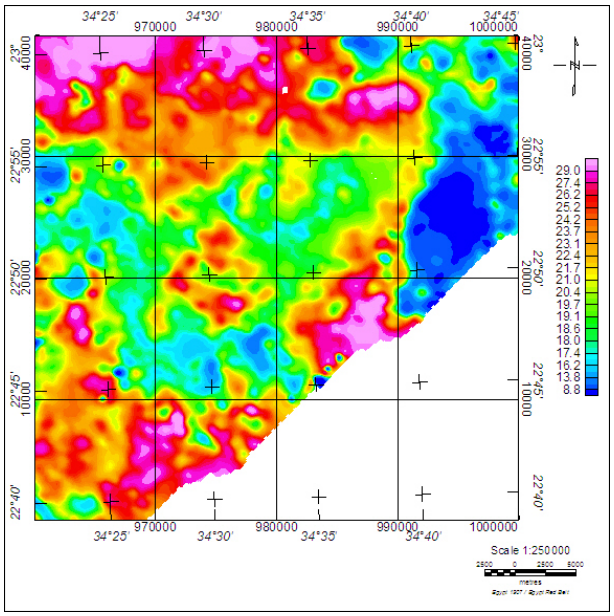

Fig. (4) Potassium map of the studied area.

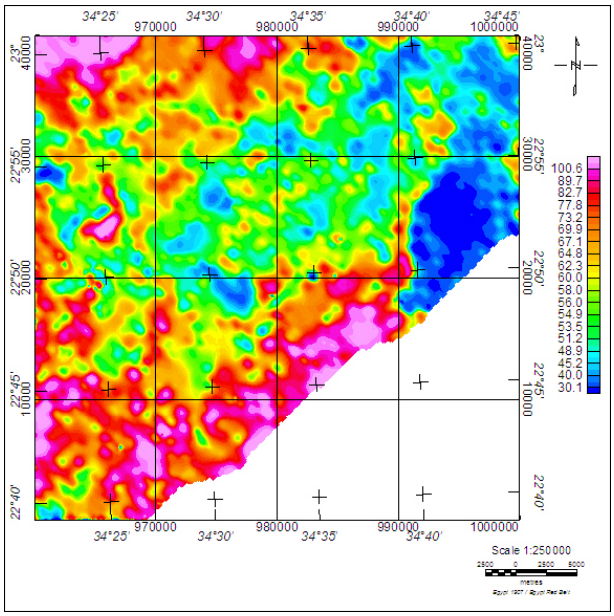

Fig. (6) Thorium map of the studied area.

Reduction to the north magnetic pole was performed at the first stage of processing of aeromagnetic data (Fig. 8).

The azimuthally averaged logarithmic power spectrum was computed (Fig. 9). The log spectrum shows two parts, where the spectral slope technique was applied to each. Isolation of the magnetic anomalies using Gaussian regional / residual separation filter was conducted for the reduced to magnetic pole map into deep-regional and shallow-residual components. The interactive spectrum technique was applied to each of them. The residual map (Fig. 10) exhibits the local anomalies, which reflect the near-surface structures, while the regional map (Fig. 11) reflects the broad anomalies related to the deep-seated changes in the composition of the Basement rocks.

The Gaussian filter is excellent for applying a straight forward high pass and low pass application. Forward modeling using the GM-SYS software package was applied only to the El Naqa ring complex. A 2-D model was used to account for the limited extent of the intruded zone perpendicular to the flight lines. The magnetic response of the model was then calculated for comparison with the observed aeromagnetic data (Fig. 12).

Landsat Enhanced Thematic Mapper plus (ETM^+) data of the studied area were processed for surface geological and structural mapping. The studied area was collected from Landsat-7 of ETM^+ scene date 2001 of Path 173 and Row 44. The digital image processing technique has been applied to the ETM^+ data covering the study area using ERDAS Imagine 9.1 software.

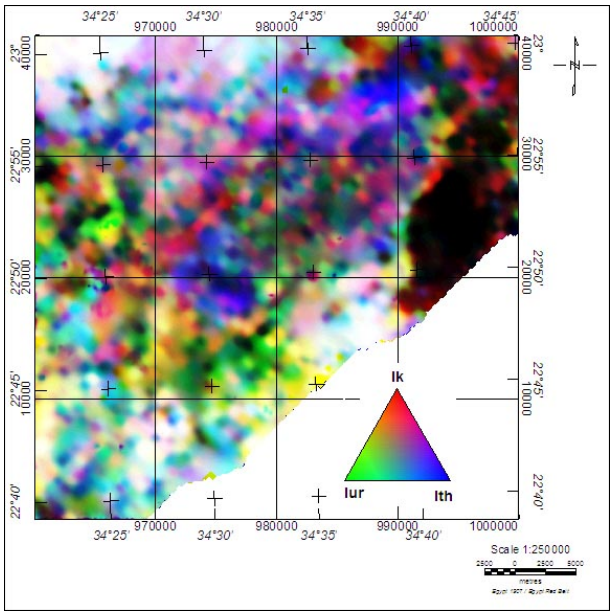

Fig. (7) Linearly/stretched false color radio-element ternary image of the studied area.

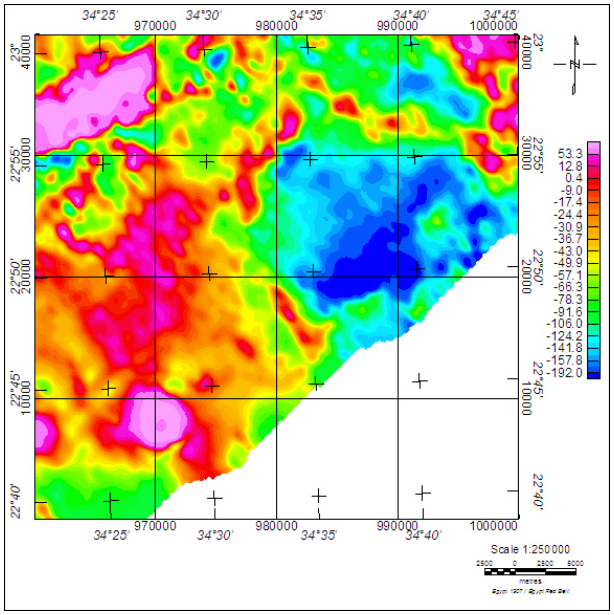

Fig. (8) Total intensity magnetic map, reduced to the north magnetic pole of the studied area.

Two false color composite images of ETM$^+$ images of bands 7, 4 & 2 (Fig. 13) and ratio bands of 5/7, 5/4 and 3/1 (Fig. 14) were used for the lithological interpretation, because certain features are more enhanced in certain outputs than others. Due to the mineral contrast of mineralogy in certain lithologic units, they could not be identified distinctly in the processed images. Resampling has been made to project the produced data from UTM (Universal Traverse Mercator) system to ETM (Egyptian Traverse Mercator - Red Belt) system. This process was necessary to achieve the compatibility with airborne spectrometric and magnetic data, and to ensure the coincidence between the different layers, that could be extracted from both types of data.

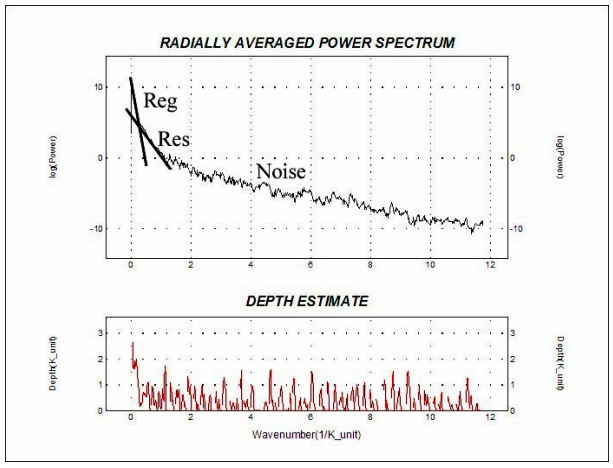

Fig. (9) A typical interpretation of the energy (power) spectrum with the average depths to the deep and shallow sources.

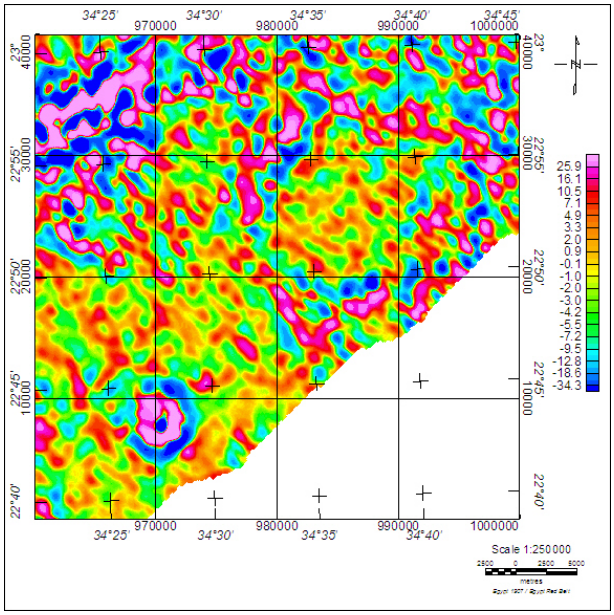

Fig. (10) Residual magnetic component map of the studied area.

Discrimination of Rock Types:

The purpose of this study is to look at the airborne spectrometric, magnetic and remote sensing data to discriminate the rock types of the study area. There are many features such as the geologic contacts, color, lineaments and dike swarms, as well as the photogeologic characteristics encountered in the rocks, can be used for investigating bodies of lithologic units.

Airborne Spectrometric Data:

The survey data cover approximately two thirds of the study area. The qualitative analyses of the spectrometric and magnetic data have led to discriminate between the acidic and intermediate rock types over this entire area. The older and younger granites occupy much of the area. The outcrops of the older granites are generally poorly enhanced by the spectrometric data. To the southeastern part of the surveyed area at G. El Waqif, the correlation between

the mapped gniess and schist and the spectrometry response as recorded, becomes progressively poorer. This contrast is due to distinct positive total count, potassium and thorium with a lower extent for uranium, which reflects, gneissose granite exposures. A Cretaceous ring complex is located at G. El Naqa. This is reported as a fully differentiated complex with a complicated structure containing nepheline syenites and therefore it may be a respiratory of rare elements including uranium and thorium. This is justified, because the ring core consists of felsic rocks. Meanwhile, the survey data do not cover the area over the Mishbih ring complex.

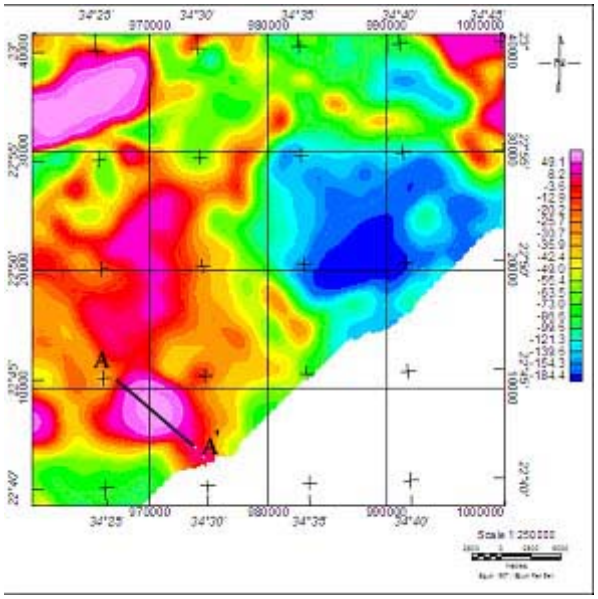

Fig. (11) Regional magnetic component map of the studied area.

Radioelement Ternary Image:

The integration of visual inspection of the ternary map (Fig. 7) and the geologic map of the area (Fig. 2) reveals a remarkable contrast between the mapped exposures of the predominant rock types in the southeastern part of the surveyed area and their spatially associated score values. Gneiss and schist at G. El Waqif in the mapped geology display high radiometric responses (parts of white color) clearly identified on the ternary image. It can be easily discriminated as acidic rocks (gneissose granite) and differentiated from the basic rocks (parts of black color), which show low radioactivity levels, The G. El Naqa ring complex shows high K%, eU and eTh background levels, and should be considered a good target for exploration followup. It can be identified by its distinct high response of potassium, uranium and thorium, except over the outcropping ring complex. The relative increase of eU concentration levels (the change in color from white to green) can be attributed to the potential leaching of eU element from the high topographic exposures and transported to the low relief parts. The rapid change in color from white and pink to black and magenta indicates a change in rock the types with low radioelement concentration levels (metasediments, metavolcanics, and granodiorites). The older granites are displayed in various colors. This color variation may be due to different grades of rock alteration associated with the redistribution in radioelements concentrations, as well as, the presence of radioactive minerals.

Airborne Magnetic Data

The surface geology displays outcropping of Basement rocks. It seems to be divided magnetically into two zones, as shown from the total intensity magnetic map reduced to the north magnetic pole (Fig. 8). The western portion displays high amplitude anomalies than the eastern part. There is apparently a geochemical change in the Basement complex as a whole, with similar rock types mapped on either side of the boundary displaying the change. Also, the mapped younger granite at the northwestern side of the area appears to be magnetically transparent with a possibly deeper magnetic source below it.

Visual inspection of the total intensity magnetic map reduced to the north magnetic pole (Fig. 8), with the residual (near-surface) and the regional (deep-seated) components maps (Figs. 10 and 11) reveal strong positive anomalies over the El Naqa ring complex. The positive magnetic anomaly is circular in the plane view and centered on the mapped outline of the complex. The magnetic high reaches a maximum at the center of the intrusion, where mapping shows the thickest nepheline syenites sheets. This is reasonable, since the compositions of the El Naqa ring complex indicate a mantle source for the magmas. In simple terms, it consists of three concentric zones. An increase in the degree of intrusion with depth could reflect a greater ease of emplacement in the ductile crust, but it may also be the cumulated effect of multiple cycles of magma recharge as suggested by the emplacement sequence of units at surface. The residual magnetic component map suggests that, subvertical contacts extend to midcrustal depths with more information and predictions about the downward continuation of ring complexes through the lower crust from the regional magnetic component map.

The magnetic response of the crustal model is based on the magnetic susceptibility contrasts given in Figure 12. The intruded zone beneath El Naqa ring complex is geometrically well defined by the concentric magnetic anomalies. Many intrusions are likely to be subvertical dikes since, the dikes are thought to represent the most effective form of magma transport through the crust. The important point is that, the crust under El Naqa ring complex is perversely intruded throughout a zone whose width is nearly the same at all depths.

The anomaly flanks are steep and coincide with the ring rim. Thus, the magnetic anomalies are centered precisely on the surface expression of El Naqa complex and coincide with its diameter at the level exposed.

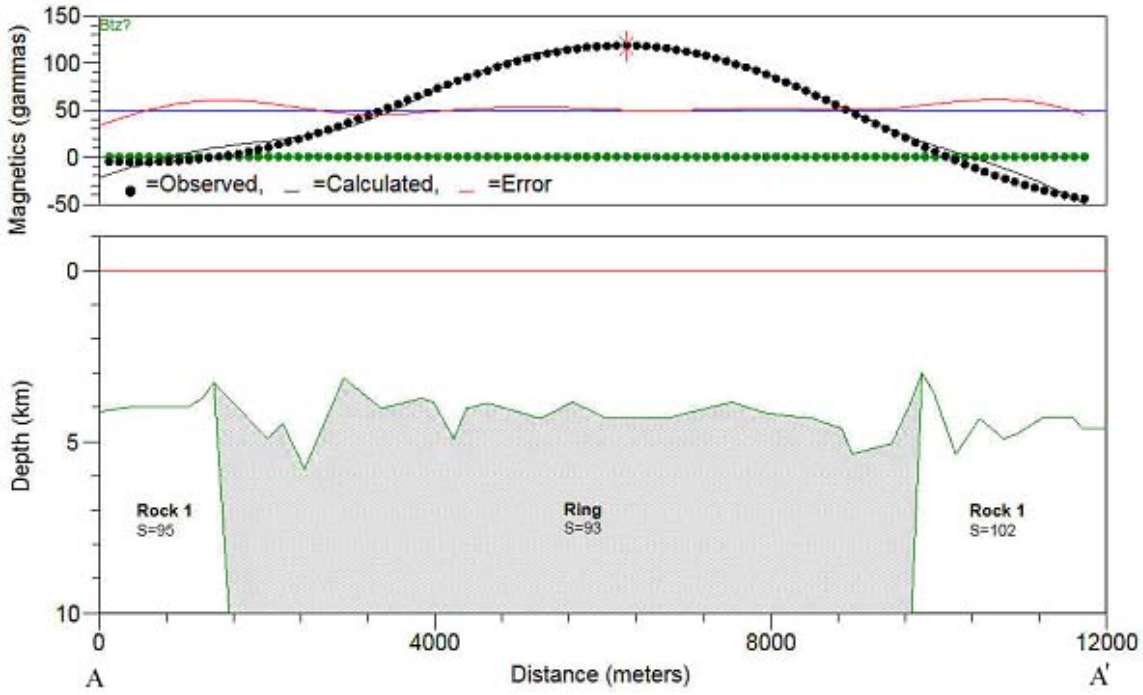

Fig. (12) A 2-D magnetic model of the crust beneath El Naqa ring complex. Geometry and Susceptibility of the model are constrained by the geology of the complex for the uppermost layer.

From their sharp magnetic contrast, the intrusion is assumed to have steep discordant contacts with the enclosing rocks and to be cylinder in shape. The size in plane view as inferred from magnetic maps is 8 km in diameter. The near-constant diameter of the complex at all depths is the most striking feature of our crustal model and it could not have been predicted from surface studies or from the classic concepts of ring complexes.

LANDSAT ETM$^+$ IMAGERY

False Color Composite (FCC) Image

From the interpretation of false color composite images of ETM+ bands 7, 4 & 2 (Fig. 13) in RGB, we can discriminate the boundary of rock units, according to the color differences and photogeological characteristics of rocks. Quaternary deposits (Q) have plains and Wadies of very light blue to pale yellow color. These rocks, except at the basin margin to the north, are mostly flat lying or gently dipping. This poorly sorted mix of debris contains a fine matrix enclosing outsized pebbles, cobbles, boulders and sometimes rock types. Two ring complexes have oval to circular shapes and reddish brown color, sharp ridges, high relief, and sharp contacts with the surrounding rocks.

The two ring complexes lie in the extreme south of the study area (Fig. 2) and form a group of hills rising from an almost level plain developed on the Basement rocks.

Meshbeh and El Naqa ring complexes composed mainly of acidic and intermediate volcanics, syenites and per-alkaline granites, have closer affinities to these complexes than to the main part of the host rock province, where biotite-granites are the most abundant rock type. Gneissose granite has an elongated foliated outcrop with bright or light brown colors; older granites have light brown color with low relief and high fractures, and high dike swarms. The metasediments and metavolcanics are conspicuous on this image by a very dark tone indicating relatively strong absorption for both the near infrared and visible bands.

Statistical analyses of these lineaments revealed that the predominant structural trends affecting the study area are arranged in decreasing order, as NE-SW and NW-SE. This correspond to data by Mansour (1996) which revealed that the intersections between the NW and NE trends, in several cases, control the distribution of radioactive mineralization. Spatial integration of the various data sets including previous works, Landsat ETM$^+$ image and airborne spectrometric and magnetic data were used for investigating the lithological discrimination and the regional structural lineaments crossing the area, as well as to delineate the anomalous zones in the study area.

The predominant lineaments are running conformably with both the main local geologic structural features manifested in the area of study and with the regional structural trends of the southern Eastern Desert of Egypt.

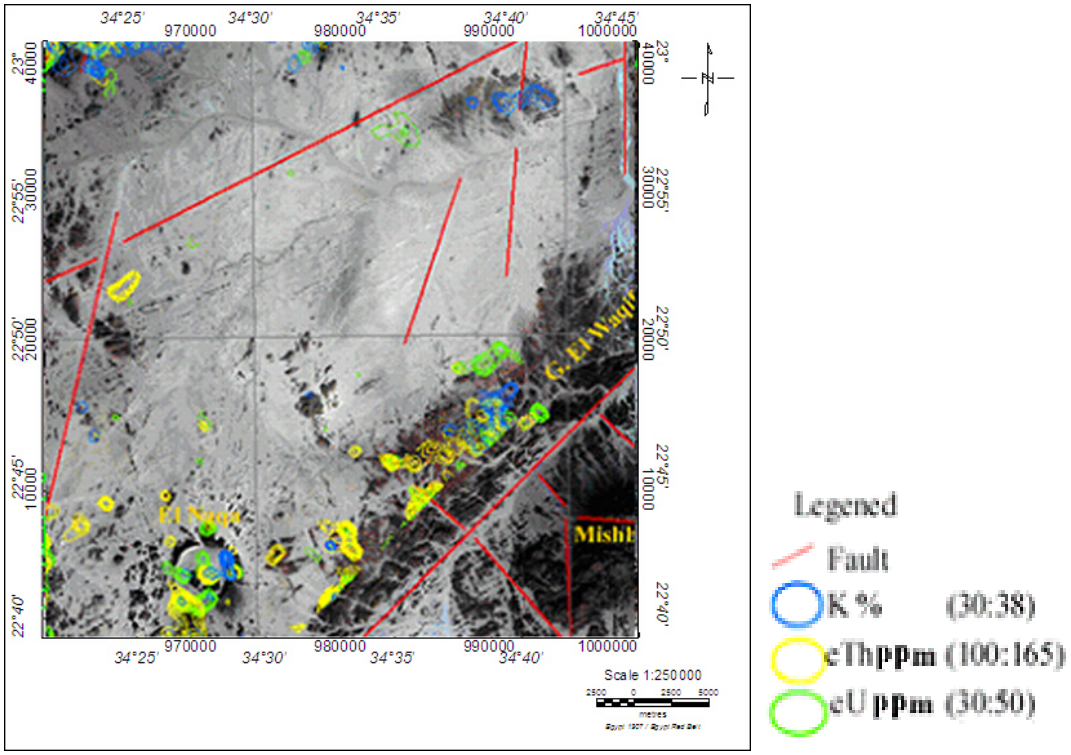

Fig. (13) False color composite image (bands 7, 4, 2 in RGB) with structural trends and locations for radioactive anomalies zones in the studied area. (Map values in units of One Tenth of 1 ppm eU / ppm eTh / K percent)

There is a major fault separating G. El Waqif and Mishbih ring complex, which trend in the NE direction, where some zones of radioactive elements occur along this structural fault, as shown in Figure 13. Also the ring complexes are considered as the main target for radioactive elements, which are of very high interest for anomalies. The radioelements in the mapped area have three high anomalous zones as in Figures 7 and 13. The first along the main structural fault at Mishbih ring complex and G. El Waqif, while the second is at the northwestern corner of the study area, which contain very high anomaly values, finally at El Naqa ring complex.

Spectral Characterization

The spectral profile viewer of the image processing software allows a user to visualize the reflectance spectrum of a single pixel through many bands. This technique is particularly useful for multispectral data, that have several layers. It allows estimating the chemical composition of the material in the pixel. The spectral reflectance curve for each of the 7 widely exposed rock units were extracted from visible, near infrared and short wave infrared ETM+ data. For each rock unit, the spectral reflectance curves were extracted from different locations and compared (Fig. 14). Table 1 shows the differences in the measured reflectance values DNs in the 6 bands for all the exposed rock types in the studied area. The shape and pattern of the spectral curve of any rock type is mainly dependant on its mineral composition.

According to the visual interpretation of spectral reflectance curves, it was found that, the spectral reflectance curves of the 7 rock units show decreasing reflectance values in the transition from wavelength regions (0.53 – 0.61 µm and 0.75 – 0.90 µm), corresponding to the ETM+ bands 2 and 4, respectively. It shows that the ring complex, metavolcanics and matasediments have low reflectance values, while the older and younger granitoids rocks show high reflectance values. These values, to some extent show the relative amount of the absorbed minerals e.g. Fe, Mg oxides in amphiboles or mica, as well as the reflected minerals, such as silica and feldspars among these rocks. Also, it has been found that, the spectral reflectance curve for the gneiss and schist (in the mapped geology) at G. El Waqif shows a spectacular unique behavior compared to the spectral reflectance curve for the younger granite in the northwestern side of the area. This reveals that, it can be discriminated by the spectral reflectance curves as the gneissose granites. This correlates well with the airborne spectrometric and magnetic data, where they reflect a distinct high total count, potassium and thorium, with a lower count for the uranium and appear to be magnetically low. In contrast, the highly weathered older granites produce high reflectance and tend to show up light tone color pattern of dull and light brown.

These rocks are detected on the false color composite ratio image by blue to violet tone, which is symptomatic of the presence of altered clays and other hydroxyl minerals.

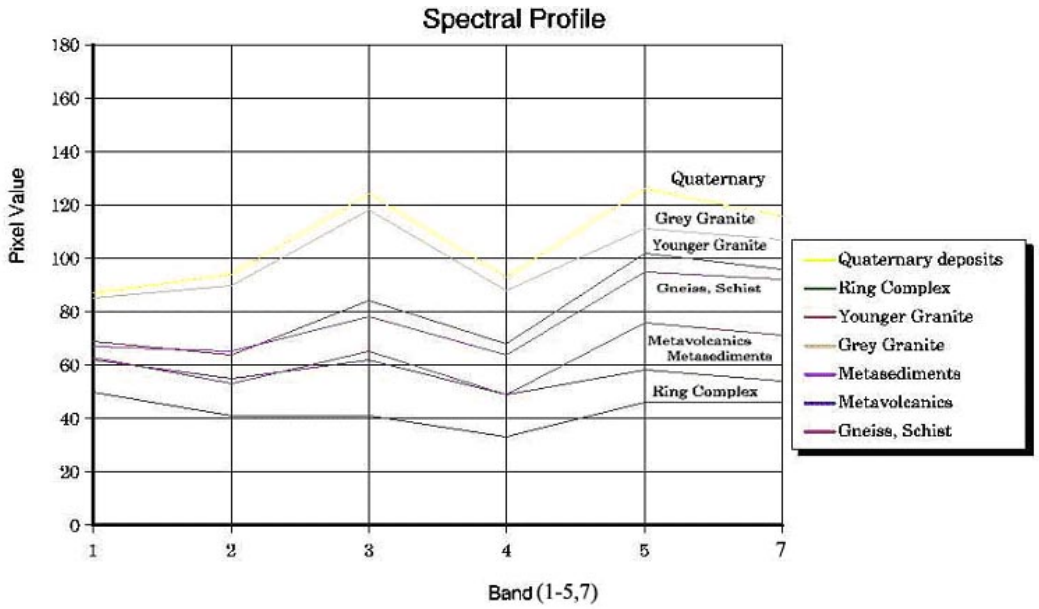

Fig. (14) : Spectral characteristic curves for the different rock units exposed in the studied area.

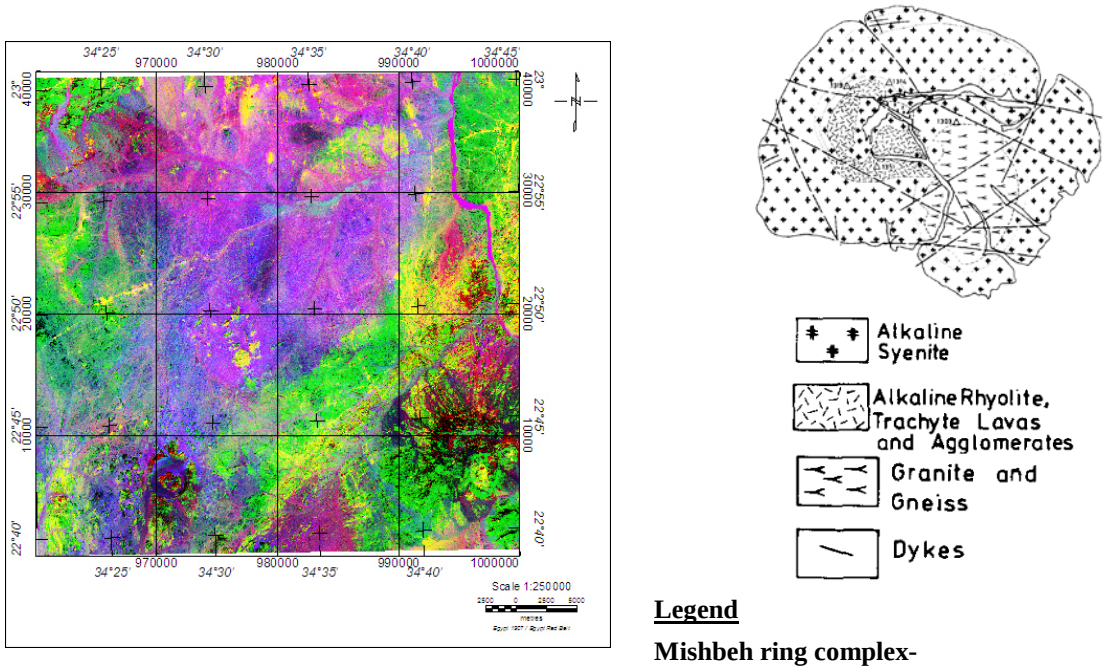

Legend

Mishbeh ring complex-
after El Ramly & Hussein (1985).

Fig. (15): False color composite ratio image (5/7, 5/4, 3/1 in RGB) of the studied area.

Table (1): Pixel values of the examined Basement rocks in different spectral bands of the studied area.

Rock Units	Band (1)	Band (2)	Band (3)	Band (4)	Band (5)	Band (7)
Quaternary Deposits	90	95	122	95	128	117
Ring Complex	51	41	41	37	48	48
Younger Granite	70	66	82	71	102	97
Grey Granite	88	90	118	90	110	107
Metasediments	62	53	63	50	58	50
Metavolcanic	62	52	65	50	76	70
Gneiss & Schist	69	65	79	68	97	94

False Color Composite Ratio Image

The false color composite ratio image (5/7, 5/4 & 3/1 of landsat ETM+ image in RGB) was used for the discrimination of the different Basement rocks exposed in the study area (Fig. 15). Although this combination of ratio image appears to be some what different from the false color composite image, the final result remains the same, thus lending support to the previous conclusion. Using the theoretical knowledge about the spectral properties of most rocks and minerals, ETM+ bands 3/1 and 5/7 were selected for the iron oxides and hydroxyl-bearing mineral, respectively, whereas the band ratio 5/4 has been computed to enhance the possible ferrous oxides. Rothery (1987), Drury and Hunt (1989) and El Rakaiby (1996) denoted that, the ETM+ bands 1 to 4 contain information about iron minerals. The obtained image has mapped the alteration zone in reddish yellow.

This alteration can easily be observed in the right central part of the image. Quaternary deposits are represented by light violet to pinkish blue toned color due to the high reflectance, but they have low relief due to their residence at low land and wadies. Ring complexes lie at the southern part of the study area and have light yellow to orange toned color at the outer parts, while the core exhibit pale green to dark blue and display cone to circular shapes. The gneissose granites at G. El Waqif (gneiss in the mapped geology) and the younger granites at the upper left corner show green to light green toned color due to the medium reflectance and absorption, but most of them are highly deformed, of moderate elevation, and are parallel in drainage tributaries. The older granitic rocks are represented by light pinkish to pale blue toned color, highly fractured and high in elevation, and are rectangular in drainage pattern. The metavolcanic rocks and flanks of the ring complexes are represented by reddish to dark red color, where this darkness is due to high absorption of electromagnetic waves. Most of the volcanic area shows massive appearance and circular elevated shape, as well as angular drainage pattern.

El Ramly & Hussein(1985) described the Mishbeh ring complex as a relatively large complex, about 10 km across and is built up of an outer thick ring-dike of alkaline syenite, enclosing four smaller ring masses within. The ring nature is only indicated by the ring fracture and the whole of Mishbeh is essentially a mass of alkaline syenite. Remnants of the volcanic cone are preserved only in the northwestern part of the complex and are represented by agglomerates of trachytic composition. The southeastern inner ring structure has a core of country rocks enclosed within the syenite dike.

SUMMARY AND CONCLUSIONS

The gneiss and schist at G. El Waqif can be discriminated as gneissose granites. They show elongated foliated outcrops with bright or light brown colors from the landsat image. This is correlated well with the airborne spectrometric and magnetic data, where they reflect a distinct high total count, potassium and thorium, with lower count for uranium that appears to be magnetically low. The radioelement ternary map of K, eU and eTh (in RGB) provides only one display of overall picture of the radioelement distributions in the study area. This map offers much in terms of lithologic discrimination based on the color differences and photogeologic criteria. Isolation of the magnetic anomalies using Gaussian regional-residual separation filter was conducted for the separation of the reduced to magnetic pole map into deep regional and shallow residual components. The magnetic interpretation for the El Naqa ring complex demonstrates that the 2-D structure of ring complexes is not restricted to the brittle upper crust, but can extend through the crust as well. The near-constant diameter of the complex at all depths is the most striking feature of our crustal model and it could not have been predicted from surface studies or from the classic concepts of ring complexes. The airborne spectrometric and magnetic data do not cover the area over the Meshbeh ring complex. The landsat imagery technique points out the fact that, when airborne spectrometry and magnetic survey data are not available, ETM^{+} imagery can produce good results in differentiating rock units. Two ring complexes appear at the southern part of the study area in the landsat imagery, and have cone and circular shapes. Statistical analyses of the surface structural lineaments revealed that, the predominant structural trends affecting the study area are arranged in a decreasing order as NE-SW and NW-SE and E-W.

REFERENCES

Abdel Monem, A.A.; Hussein, H.A.; El Amin, H.M.; Mansour, S.I. and El Afandy, A.H., (1998): Contribution to the geology and geochemistry of Hadayib ring complex, South Eastern Desert, Egypt. The Mineralogical Society of Egypt, Geol. & Geophys. Sciences Department, National Research Centre, Dokki, Cairo, Egypt, Vol. 10, pp. 249- 264.

Aero-Service (1984): Final operational report of airborne magnetic-radiation survey in the Eastern Desert, Egypt, for the Egyptian General Petroleum Corporation. Aero-Service Division, Houston, Texas, April 1984, six volumes.

Bowden, P., (1985): The geochemistry and mineralization of alkaline ring complexes in Africa (a review). Journal African Earth Sciences 3, 17-39.

Conoco Coral Corporation and The Egyptian General Petroleum Corporation (1986): Geological maps of Berenice and Hamata.

Drury and Hunt, (1989): Geological uses of remotely sensed reflected and emitted data of Laterized Archean terrain in Western Australia. International Journal of Remote Sensing, Vol. 3, pp. 345- 497.

El-Gaby, S., List, F.K., Tehrani, R., (1990): The Basement Complex of the Eastern Desert and Sinai. In: Said, R. (Eds.), The Geology of

Egypt. Balkema, Rotterdam, Brookfield, pp. 175-I 84.

El-Nisr, S. A. and Saleh, G. m., (2001): Geochemistry and petrogenesis of the Late Jurassic- Early Cretaceous Mansouri ring complex, South Eastern Desert, Egypt. Journal of African Earth Sciences, Vol. 32, No. 1, pp. 87-102.

El Ramly, M.F. and Akkad, M.K., (1960): The Basement Complex in the Central Eastern Desert of Egypt between Lat. 24^0 30` and $25^0$ 40` N. Geol. Surv., Paper 8, 35 p.

El Ramly, M. F.; Budanov, V. I.; Hussein A. A. and Derenluk, N. E., (1970): Ring Complexes in South Eastern Desert of Egypt. In: Studies of some mineral deposits of Egypt. (ed. By Osman Moharm et al.), Geol. Surv. Egypt, pp. 181-194.

El Ramly, M. F.; Budanov, V. I. and Hussein, A. A., (1971): The alkaline rocks of South Eastern Egypt. Geol. Surv. United Arab Republic (Egypt), Paper 53, 111 p.

El-Ramly, M. F., (1972): A new geologic map of the Eastern and South- Western Deserts of Egypt. Scale 1:1000.000. Annals Geological Survey of Egypt, Vol. 1, pp.1–18.

El-Ramly, M.F., Hussein, A.A., (1985): The ring complexes of the Eastern Desert of Egypt. Journal African Earth Sciences 3. 77-82.

El Rakaiby, M. L. (1996): Discrimination of igneous rocks using digital thematic mapper data in southern Sinai, Egypt. Published by Geocrato International Center (GIC), G.P.O. 4122 Hong Kong, Vol. II, No. 4, pp. 61- 69.

Farag, S.S., (1999): The Basement rocks of Gabal Felat area and its radioactivity, Southeastern Desert of Egypt. Ph.D Thesis, Fac. of Sci., Cairo University, Cairo, Egypt.

Garson, M. S. and Krs, M., (1976): Geophysical and geological evidence of relationship of the Red Sea transverse tectonics to ancient fractures. Geo. Soc. Amer.Bull., Vol. 87, pp. 169-181.

Geosoft package 2002: Geosoft Mapping and Processing System, Geosoft Inc., Toronto.

Ibrahim, M.E., (1999): Tectonic evolution and uranium potentiality of Elba ring complex, South Eastern Desert, Egypt. Egyptian Mineralogist, Vol. 11, pages 39-62. (Kamel, 1991).

Kamel, A.F., (1991): Analysis of structural lineaments and their effect on the distribution of ring complexes in south Eastern Desert, Egypt. Journal of African Earth Sciences, Vol. B, No. 2. pp. 193 - 199.Lockwood Survey Corporation (1968)

Lockwood Geophysical Survey Corporation Limited, (1968): Airborne geophysical survey conducted in collaboration with United Arab Republic and the United Nations Development Programme. Toronto, Canada.

Mansour, S.I., (1996): Factors controlling uranium mineralization, northern locality. Um Ara area South Eastern Desert Egypt. Proc. Egypt. Acad. Sci., Vol. 46, pp. 417-432.

Rothery, D. N., (1987): Improved discrimination of rock units using Landsat Thematic Mapper imagery of the Oman ophiolite. Journal of the Geological Society, London, Vol. 144, pp. 587-597.

Serensites, M. c., Faul, H., Ronald, K. A., El Ramly, M. F. and Hussien, A. A., (1979): Alkaline ring complexes in Egypt: their ages and relationship to tectonic development of the Red Sea. Ann Geol. Surv. Egypt, Vol. IX, pp. 102-116.

Vail, J.R., Almond, D.C., Hughes, D.J., Klemenic, P.M., Pool, S., Nour, S.E.M., Embleton, J.C.B., (1984): Geology of the Wadi Oko-Khor Hayet area, Red Sea Hills, Sudan. Bulletin Geology Mineralogy, Resource Department, Sudan 34, l-20.

Vail, J.R., (1985): Alkaline ring complexes in the Sudan. Journal African Earth Sciences 3, 5-16. Vail,1989).

Vail, J. R., (1989): Ring complexes and related rocks in Africa. Journal African Earth Sciences, Vol. 8, pp. 19-40.